Mass and angular momentum of simulated massive galaxies in large radii

Xufen Wu
xufenwu@ustc.edu.cn

Department of Astronomy,
University of Science and Technology of China

In collaboration with:
Ortwin Gerhard (MPE, Garching),
Thorsten Naab (MPA, Garching) and et. al.

CfA@USTC Symposium on "SMBHs and galaxies"

Backgrounds

Observations:

- a population of old, massive ($M_\star \sim 10^{11} M_\odot$) and red ETGs were already in place at redshifts $z = 2 - 3$;
- these galaxies have smaller sizes and higher densities than present-day ETGs of similar mass (e.g., Fontana et al. 2006; Ilbert et al. 2010; Cassata et al. 2011);

Simulations:

- massive ETGs grow initially through rapid star formation fuelled by infall of cold gas at $z \gtrsim 2$ → 'in situ' old stars;
- galaxies grow gradually through minor mergers, accreting old stars formed in outer haloes → efficient size evolution (e.g., Naab et al. 2009; Oser et al. 2010; Feldmann et al. 2010; Hopkins et al. 2010; Johansson et al. 2012).

Observations and simulations suggest a two-phase scinario for galaxy formation.

Backgrounds: observations in outer galactic haloes

- little stellar mass in the outer galactic haloes $\gtrsim 2R_e$,
  long relaxation time (several Gyrs)
  $\rightarrow$ preserves halo accretion history (van Dokkum 2005; Duc et al. 2011);
- outer halo stars may contain a significant fraction of the angular momentum of the galaxies (Romanowsky & Fall 2012);
- gravitational tracers to study the ETGs at large radii:
  1) mass distribution; 2) dark matter fraction; 3) potential.

Techniques:

- long slit measurements with integral-field units (IFUs): $R \lesssim 1 - 2R_e$ (e.g., Bender et al. 1994; Gerhard et al. 2001; Cappellari et al. 2006);
- two dimensional stellar kinematics from SAURON IFU : $\sim 1R_e$ (Emsellem et al. 2007, 2011);
- planetary nebulae (PNe): $\sim 8R_e$ (e.g., Méndez et al. 2001; Coccato et al. 2009; McNeil-Moylan et al. 2012);
- individual IFU pointings and slitlet masks : $3 - 4R_e$ (Weijmans et al. 2009; Proctor et al. 2009; Murphy et al. 2011).

Backgrounds: other observational techniques

Outer stellar kinematics, strong lensing and hydrostatic equilibrium of X-ray emitting hot gas:

- massive elliptical galaxies have nearly isothermal inner mass distributions,
  equivalent to flat circular velocity curves (e.g., Gerhard et al. 2001; Koopmans et al. 2006; Auger et al. 2010; Churazov et al. 2008, 2010; Nagino & Matsushita 2009);
- lower mass ellipticals have more diffuse dark matter halos (de Lorenzi et al. 2009; Napolitano et al. 2009; Morganti et al. 2013),
  the situlation is less clear, since the mass-anisotropy degeneracy is stronger, their X-ray emission is too faint and the lensing samples are dominated by massive systems.

Globular clusters (GCs) as gravitational tracer:

- Difficulty: a larger fraction of GCs may be recently accreted systems (Coccato et al. 2013).

Backgrounds: simulations

- This is the first detailed analysis of the inner and outer dynamics of a large sample of simulated galaxies

  (Wu et al. 2014, MNRAS, 438, 2701).

The simulated galaxies

42 galaxies from cosmological zoom simulations (Oser et al. 2010, 2012)

- grow through two phase scenario of galaxy formation: rapid in-situ star formation from infalling cold gas at $z \geq 2$; accreting stars from merger at $z \leq 3$;
- baryonic physics: star formation, supernova feedback, gas cooling and a redshift dependent UV background radiation;
- mass range: $[2.0 \times 10^{10},\ 3.4 \times 10^{11}]\mathrm{M}_{\odot}\ \mathrm{h}^{-1}$;
  $R_e:\ 1 - 5\mathrm{kpc}\ \mathrm{h}^{-1}$;
  few particles in the outer regions of galaxies.

Mass distribution

- The projected stellar density distributions at large radii can be fitted by cored-Sérsic functions with $n \geq 10$, larger than for typical ETGs.

$$I(R) = I_0 \exp\left\{-b_n(n)\left[\left(\frac{R'}{R'_e}\right)^{1/n} - 1\right]\right\},$$
$$R' = \sqrt{R^2 + R_0^2}, \quad b_n(n) = 1.9992n - 0.3271.$$

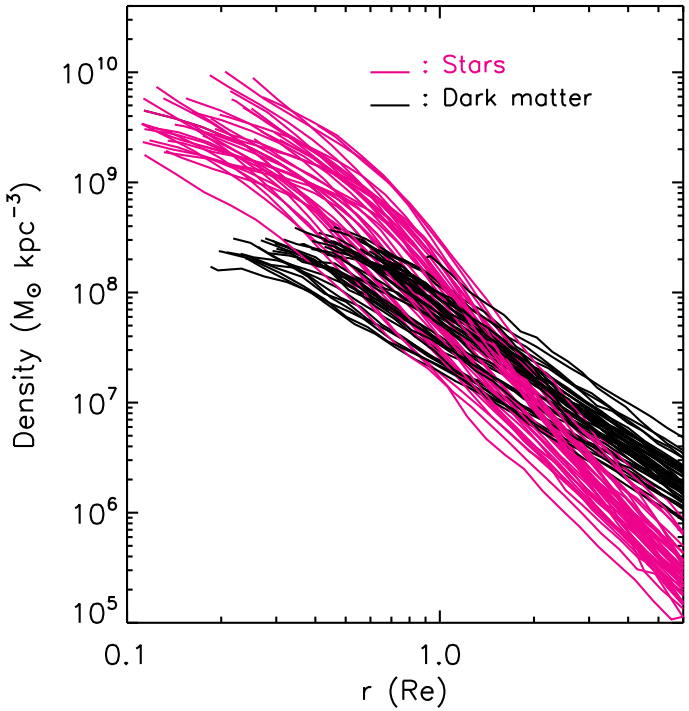

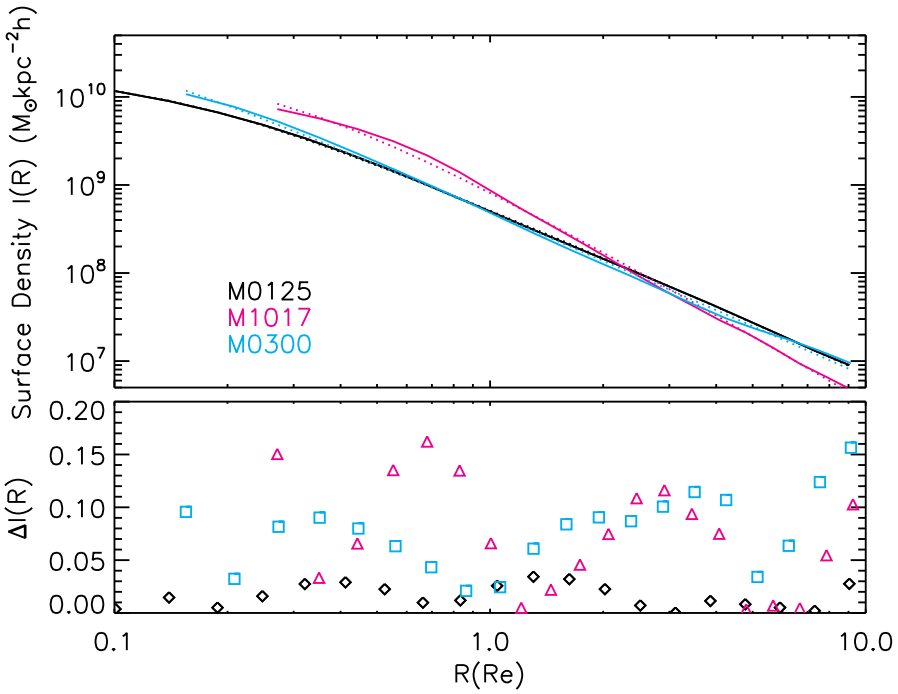

DM mass

contributions of stars and DM (blue for power-law fitting) to V_{cir} :

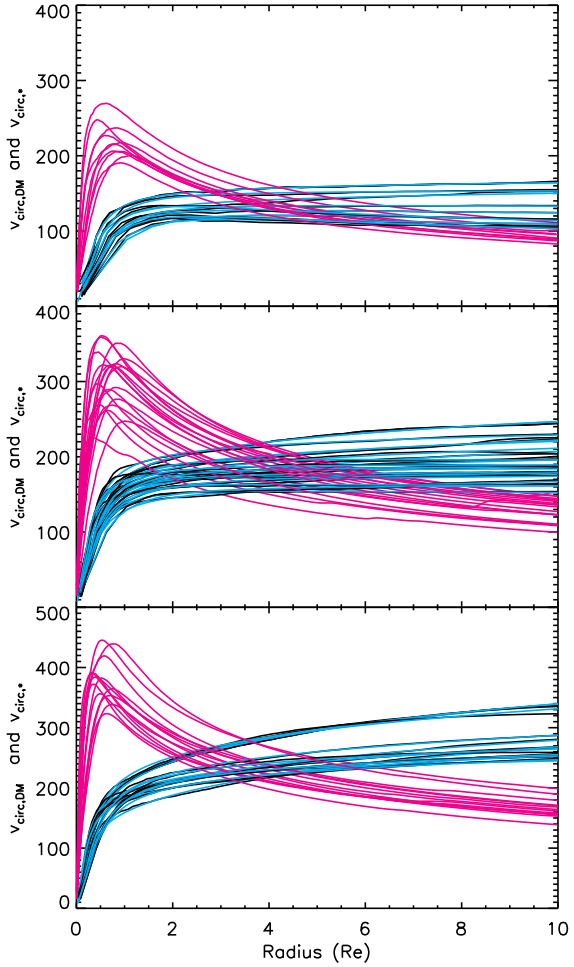

DM halo density profiles > a few kpc: simple power-law:

$$v_{\rm circ}^{\rm DM} = \frac{v_0}{(5R_e)^a} \frac{r^{1.0+a}}{\sqrt{r_c^2 + r^2}},$$

- Flat DM circular velocity curves (CVCs) for lower mass systems;
- Rising DM CVCs for high-mass halos.

Overall CVCs

Overall V_{cir}: At large radii:
Massive systems: nearly flat CVCs;
Lower mass: mildly decreasing CVCs.

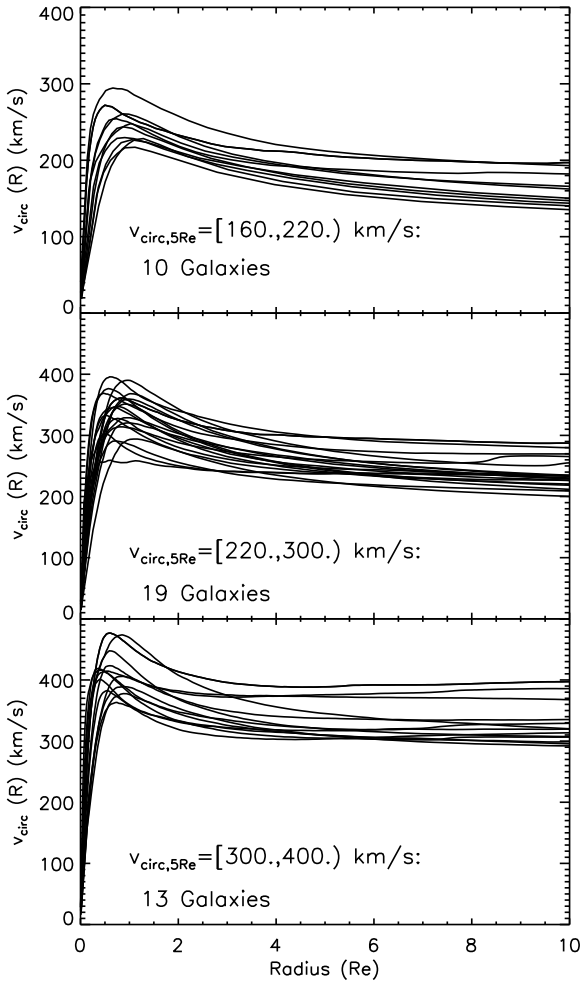

Correlations between slopes of V_{cir} and V_{cir} themselves:

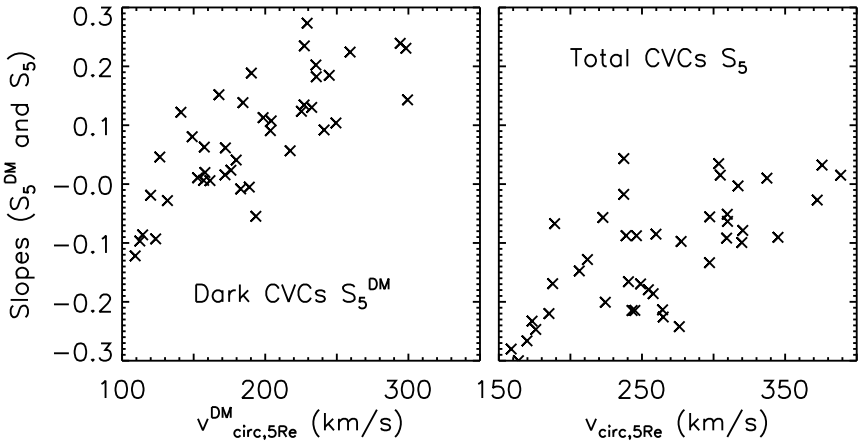

- The slope of DM CVC at 5Re correlates with DM CVC itself.
- The slope of the overall CVC (5Re) weakly correlates with CVC (5Re) itself.

DM fraction

Correlation between DM fraction, $V_{cir}(5R_e)$ and R_e

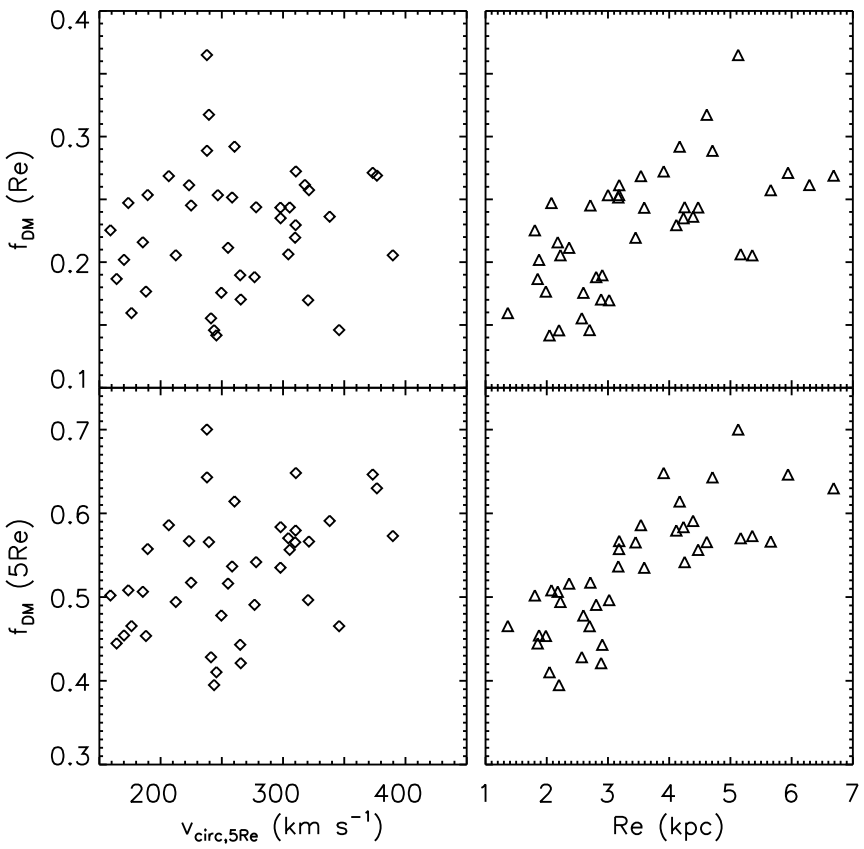

DM fraction

- $(< R_e)$: 15% – 30%; $(< 5R_e)$: 40% – 65%;
- higher in larger and more massive galaxies;
- the fractions and trends with mass and size agree with observations (Deason et al. 2012; Auger et al. 2010) .

Shape correlation and alignment

The short axes of simulated galaxies and their host DM halos are well aligned.

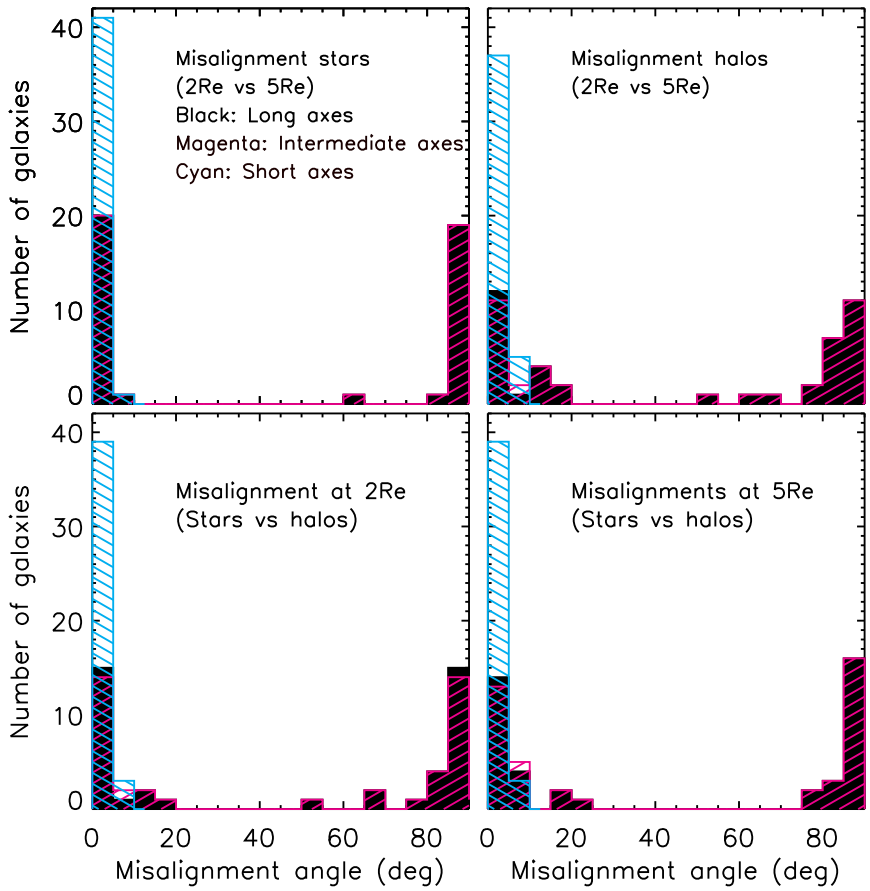

The short-to-long axis ratios are correlated.

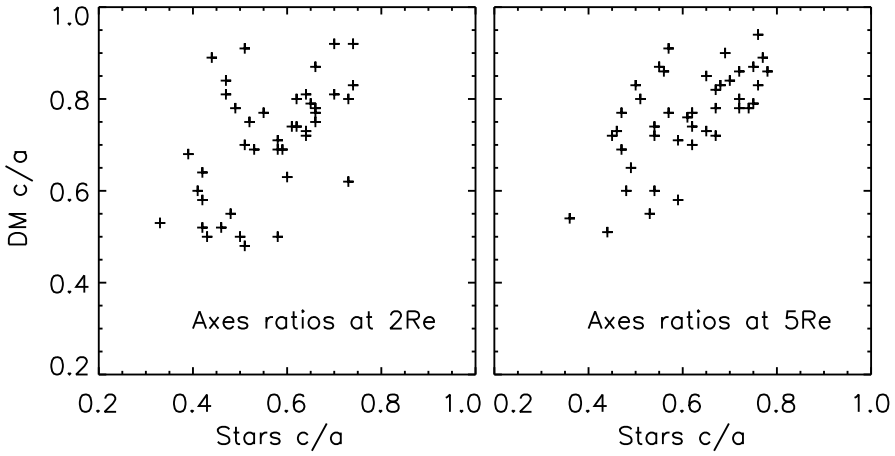

Outer kinematics - temporal smoothing method

Orbits of particles are integrated in the potentials using an spherical harmonics N-body code to reduce fluctuations caused either by particle noise or small satellites.

The LoS observables such as velocity moments, Δ_j for the $j_{\rm th}$ grid cell, are time averaged by integrating

$$\tilde{\Delta}_j(t) = \alpha \int_0^\infty \Delta_j(t-\tau) e^{-\alpha\tau} d\tau,$$

Smoothing time :$\alpha^{-1} = 200$ dts,

$$\mathrm{dts} = \frac{1}{1000} \frac{2\pi \times 10 R_e}{v_{\mathrm{circ},10\mathrm{R_e}}}.$$

(Syer & Tremaine 1996; de Lorenzi et al. 2007)

Before (upper panels) and after (lower panels) time smoothing:

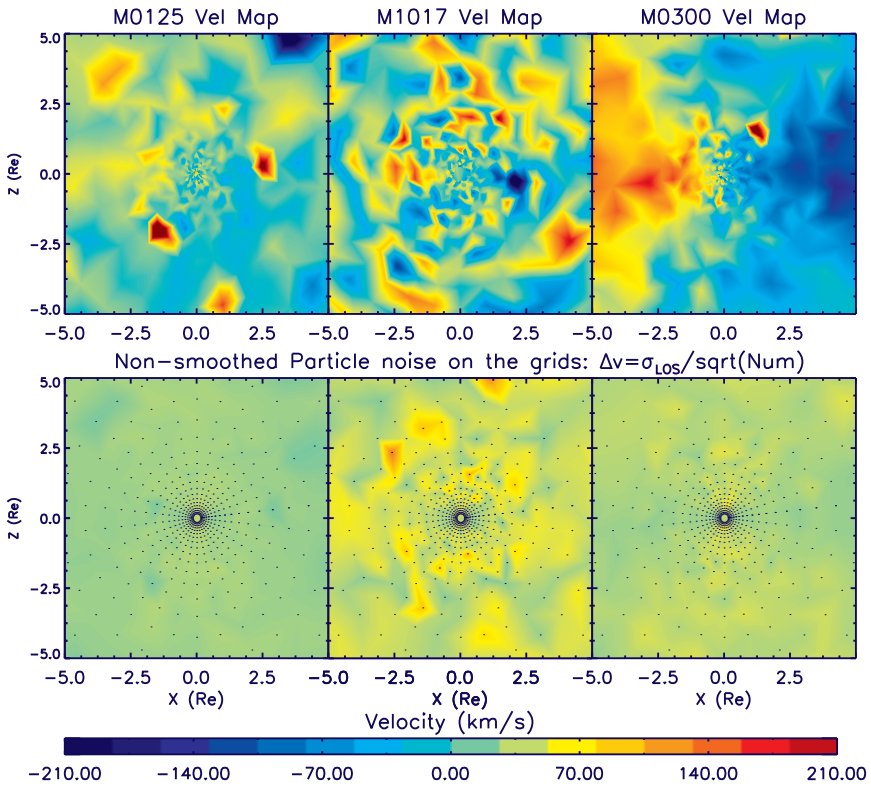

LoS kinematics

Three examples of the galaxy sample:

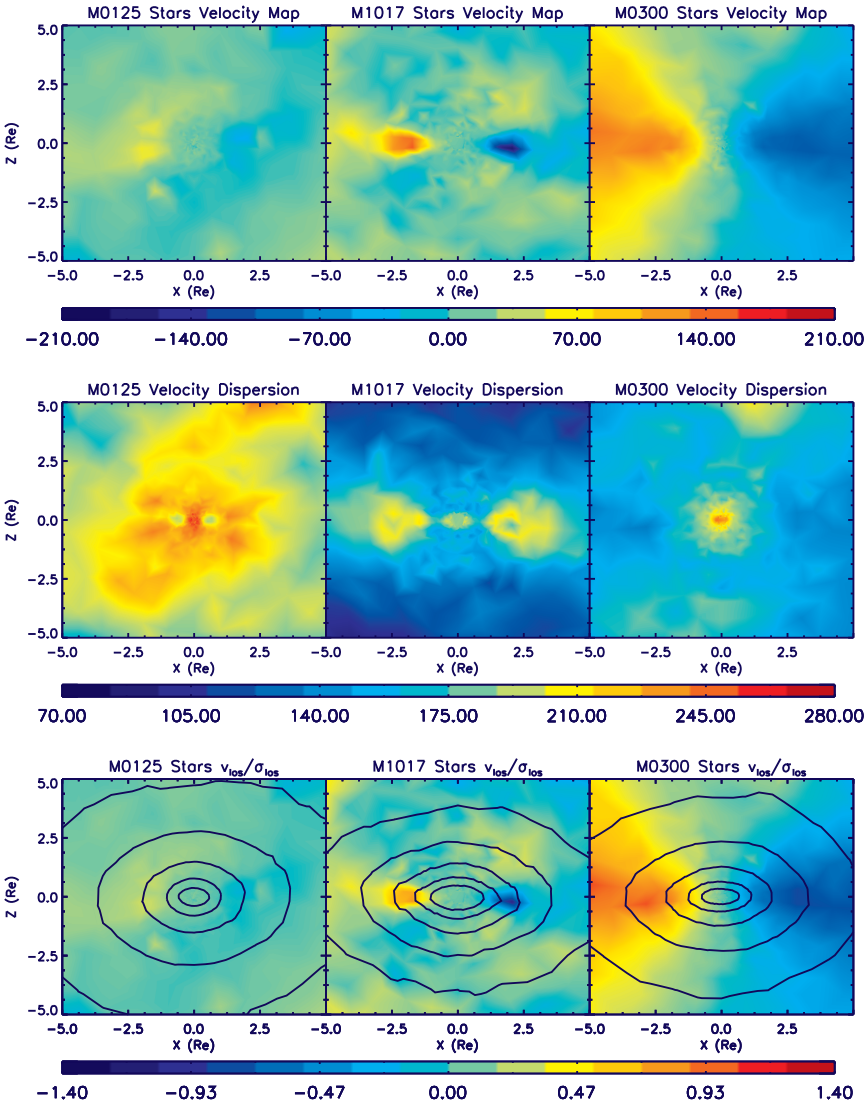

M0125 is pressure-supported;
M0300 is rotation-supported;
M1017 is mostly pressure-supported with a rotationally supported component.

Six further examples:

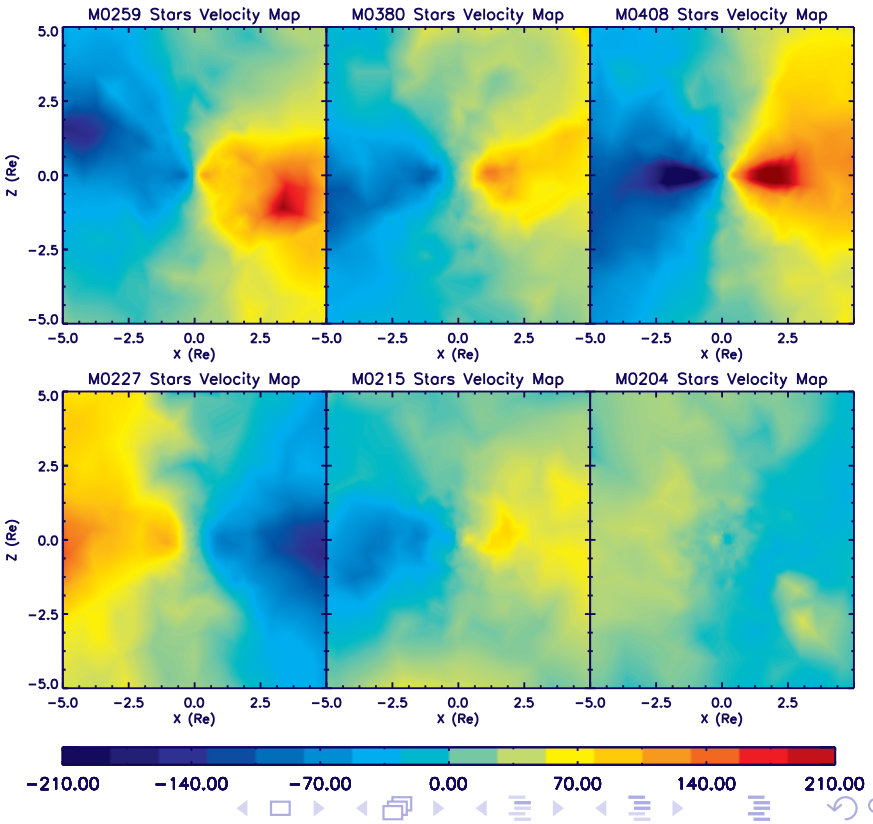

LoS rms velocity

Simulations

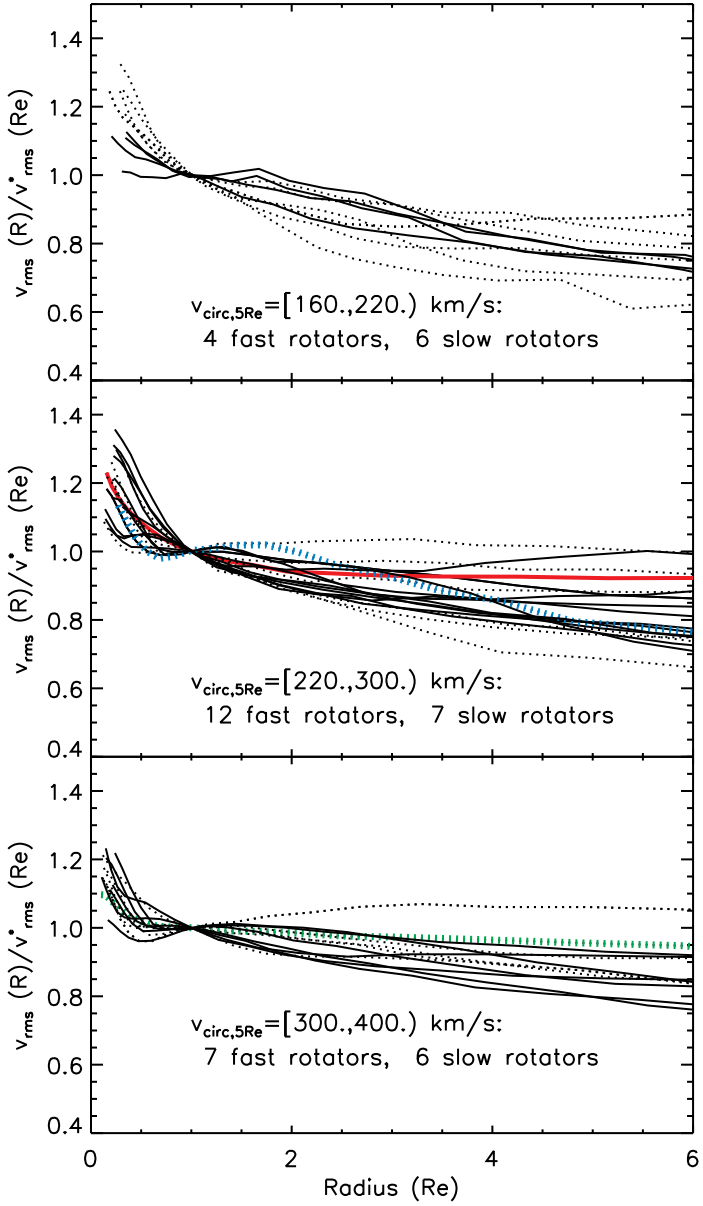

$V_{rms}(R)$ profiles are slowly declining, in agreement with the major group of PNe observations in the outer halos of most ETGs (Coccato et al. 2009), but there is no rapid falling profiles in simulations.

Observations:

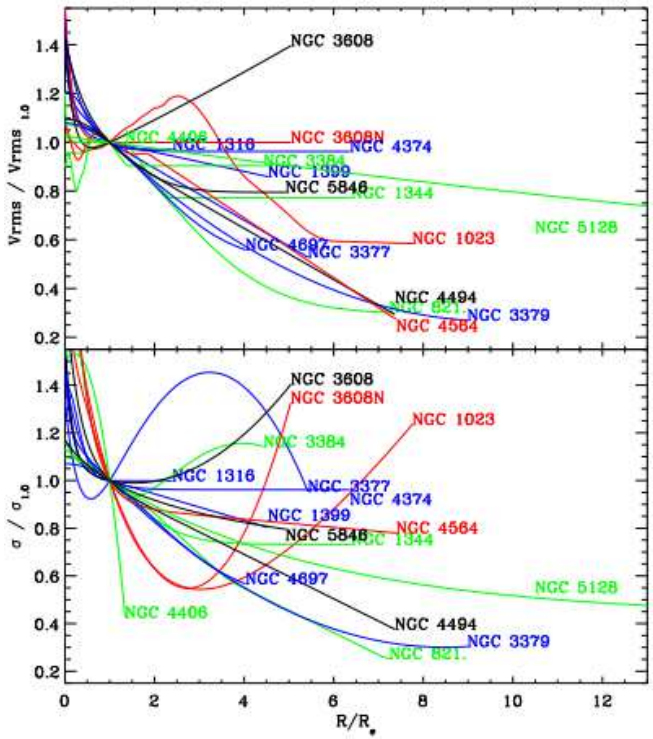

Angular momentum

Specific angular momentum:

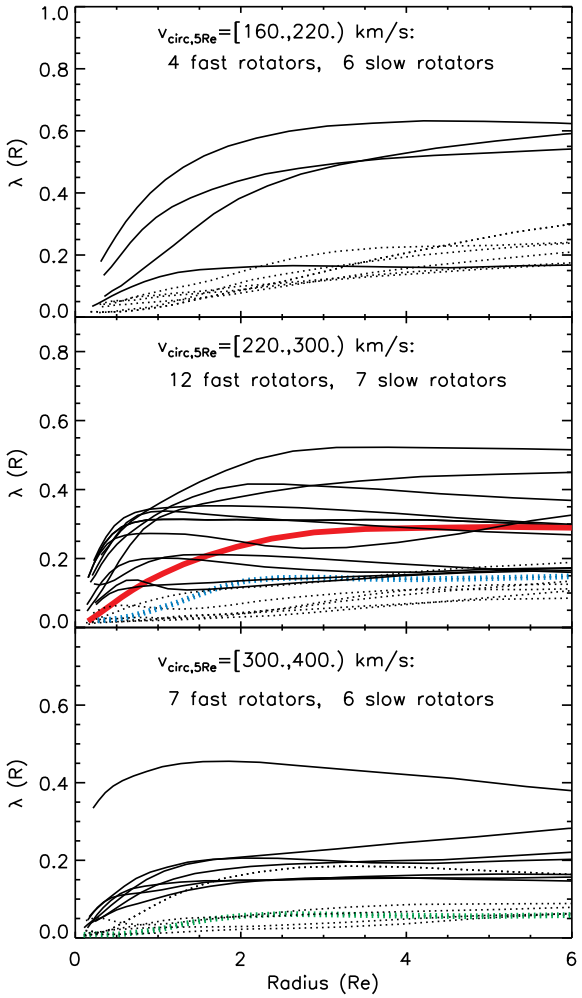

Fast rotators : $\lambda(R_e) > 0.1$, solid curves

Slow rotators : $\lambda(R_e) < 0.1$, dotted curves

Agree with observations

$$\lambda(R_i) = \frac{\sum_{k=1}^{i}\sum_{j=1}^{N_\phi} m_{j,k}^P R_k |v_{j,k}|}{\sum_{k=1}^{i}\sum_{j=1}^{N_\phi} m_{j,k}^P R_k \sqrt{v_{j,k}^2 + \sigma_{j,}^2}}$$

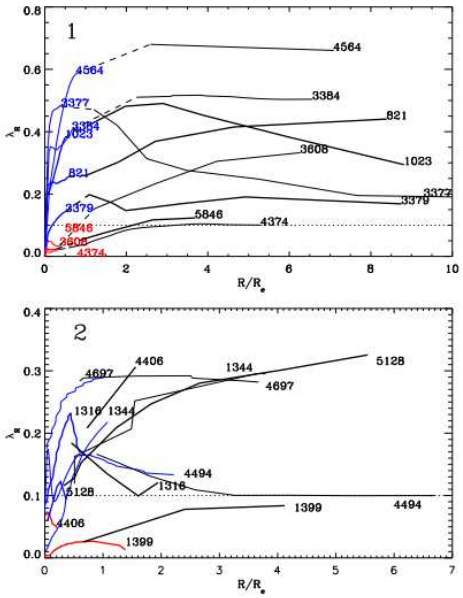

(Coccato et al. 2009)

Rotation properties are correlated at small and large radii: fast rotators rotate fast at large radii.

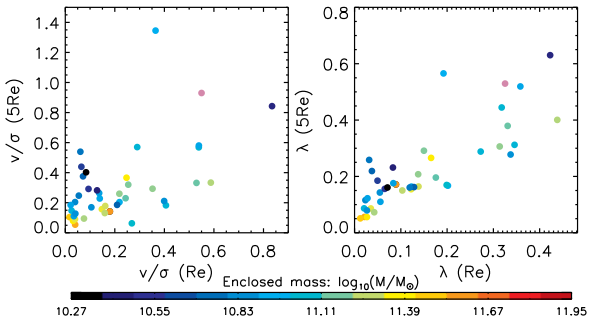

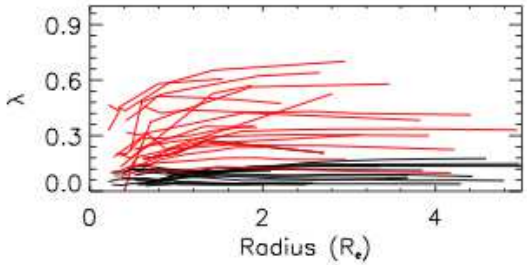

(ATLAS^{3d}, Raskutti et al. 2014)

Correlations of mass, ellipticity and angular momentum

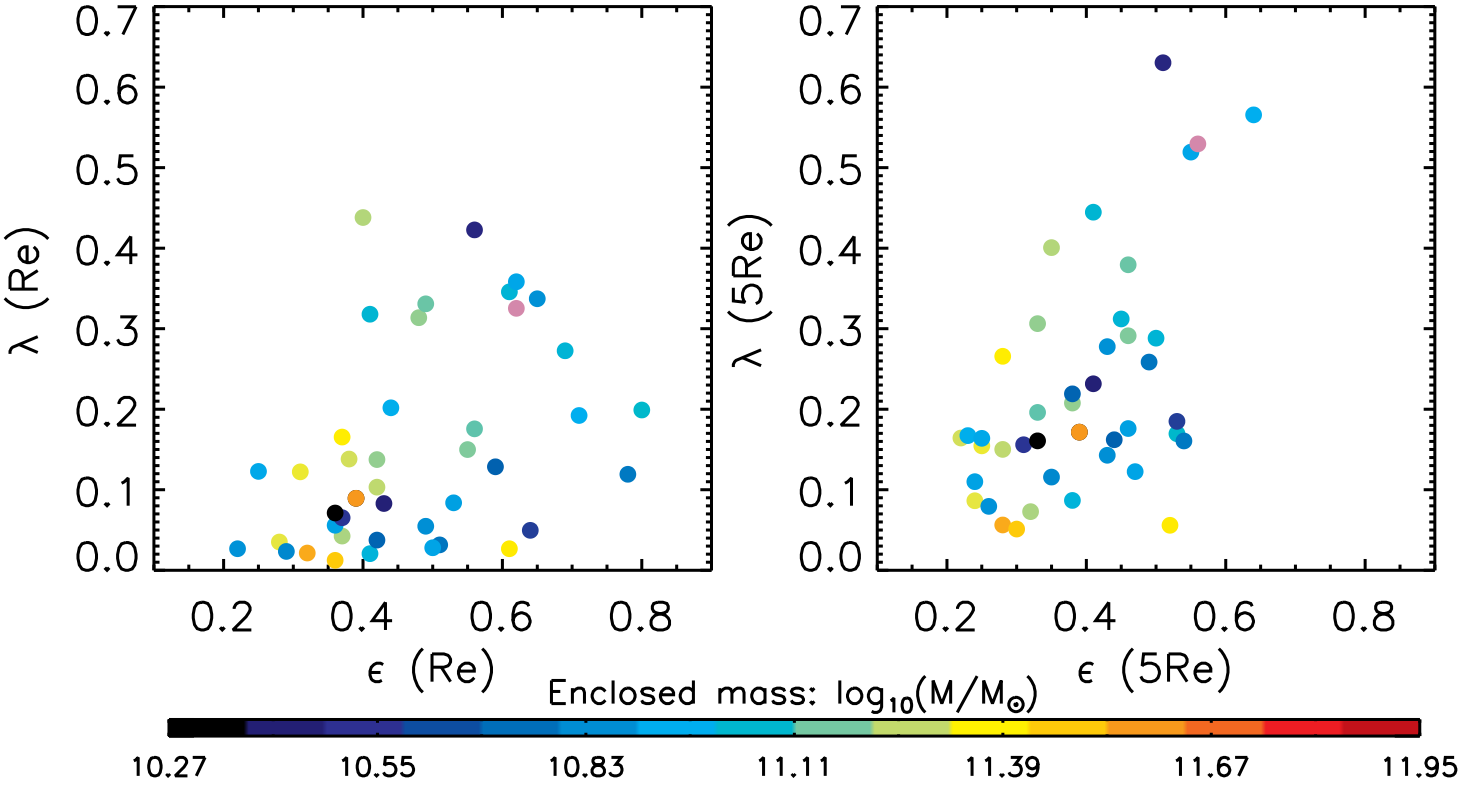

More massive galaxies have less angular momentum, and are rounder, in agreement with observations (Emsellem et al. 2011; Coccato et al. 2009).

Anisotropy profiles

Anisotropy profiles:

$$\beta(r) \equiv 1 - (\sigma_\theta^2 + \sigma_\phi^2)/2\sigma_r^2$$

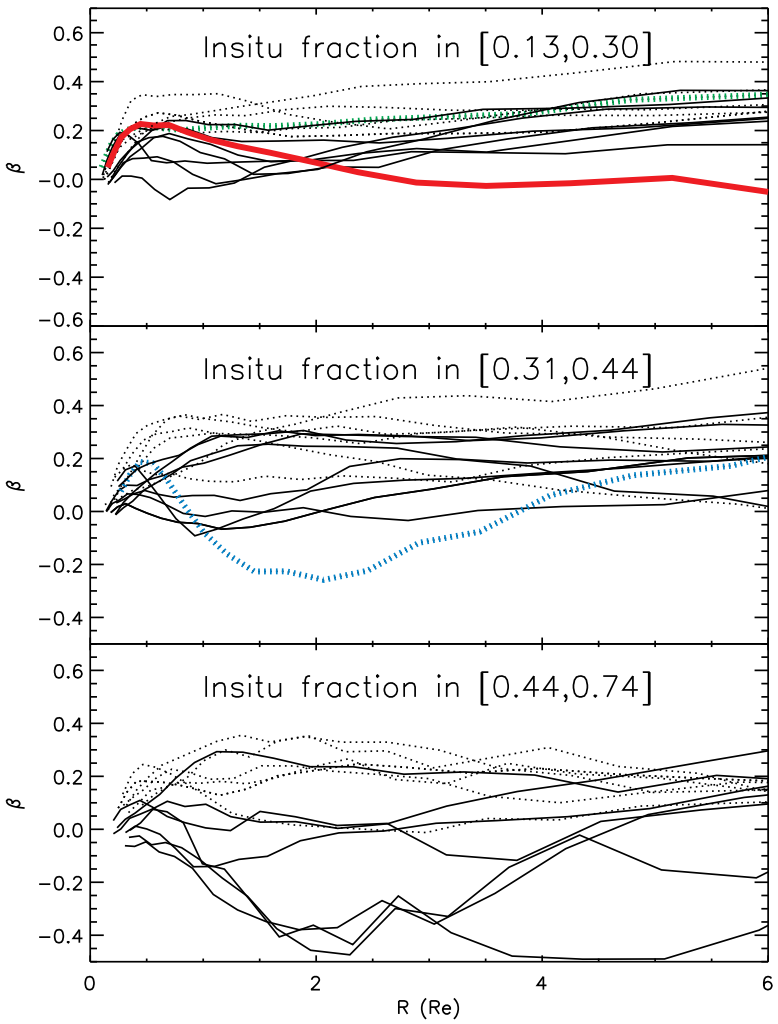

More massive galaxies with large fraction of accreted stars have radially anisotropic velocity distribution at $R > R_e$.

Tangential anisotropy is seen only for galaxies with high fraction of in situ stars.

Conclusions

- The stellar density of the model galaxies are power-law fitted well by cored Sérsic profiles with large n.
- The DM density profiles follow simple power-law. The DM CVC is flat (R^0) for less massive systems and slightly rising ($R^{0.3}$) for high mass galaxies.
- The overall CVCs are slight falling ($R^{-0.3}$) for less massive systems and flat (R^0) for more massive galaxies.
- The DM fraction is [15%, 30%] within R_e and 40% − 65% within $5R_e$. Larger and more massive galaxies have higher dark matter fractions.
- The short axes of the simulated galaxies and their host dark matter haloes are well aligned within $\lesssim 5^\circ$. througout the radial range probed ($2R_e - 5R_e$), and their shapes are correlated.
- Radial profiles of $V_{rms}(R)$ are slowly declining, independent of whether the simulated galaxies are fast or slow rotators. There are no analogues in the simulated galaxies for the rapidly falling $V_{rms}(R)$ profiles seen in the observed sample.
- For most simulated galaxies, the edge-on $\lambda(R)$- profiles are flat or slighty rising within $2R_e - 6R_e$. Most fast rotators rotate fast at both small and large radii. Overall, λ increases with ellipticity, but with much scatter.
- Simulated galaxies with a large fraction of accreted stars are generally radially anisotropic. Only systems with a high fraction of in-situ stars show tangential anisotropy.